12th IEA Heat Pump Conference 2017

Development of Steady-State Reference Model for Heat Pump System Based on Real-time Machine Learning Algorithm

Minsung Kim[a]*, Yong Soo Lee[b]

[a]School of Energy Systems Engineering, Chung-Ang University, Seoul 06974, Republic of Korea
[b]Thermal Energy Conversion Laboratory, Korea Institute of Energy Research, Daejeon 34129, Republic of Korea

Abstract

Artificial intelligence (AI) is getting more and more important in all fields of engineering technologies. Typically, thermal engineering systems are comprised of heat exchangers and fluid machinery and normally it is complicated and time consuming to analyze the systems mathematically. For heat pumps, a number of studies have been carried out to identify their operating status mathematically, however, accurate models are very difficult to develop due to numerous cases of different installation and operating conditions. Even the same heat pumps would have inevitable uncertainties by where and how they are installed. As an alternative way to estimate the performance of heat pumps, a methodology to develop a reference model using machine learning algorithm is introduced on in this study. For steady-state identification, a steady-state detector with a simple low pass filter is applied to measured signals of key features. Once steady state of the system is identified, the real-time measurements are collected to train the system model. From the study, the semi-expert based learning algorithm is effective to develop reference models of heat pump systems.

© 2017 Stichting HPC 2017.
Selection and/or peer-review under responsibility of the organizers of the 12th IEA Heat Pump Conference 2017.

Keywords: Heat pump; Steady-state; Reference model; Machine learning; Fault detection and diagnosis

1. Introduction

An increasing emphasis on energy saving and environmental conservation requires air conditioners and heat pumps to be highly efficient. In the first place, a variety of research and development on a cycle as well as its basic components have been performed to increase overall efficiency of heat pump systems. However, the efforts of the maintenance to keep the system efficiency the same as that right after installation in field were treated lesser important by manufacturer. A survey of over 55,000 residential and commercial units found the refrigerant charge to be incorrect in more than 60 % of the systems (Proctor, 2004). Another independent survey of 1500 rooftop units showed that the average efficiency was only 80 % of the expected value, primarily due to improper refrigerant charge (Rossi, 2004). To this end, various technologies were reported to analyze the performance of heat pump systems including the function of fault detection and diagnosis.

Fault detection and diagnosis is accomplished by comparing a system's current performance or parameters with those expected based on the measurements taken from the system when it was known to operate fault-free. FDD method development includes a laboratory phase during which fault-free and faulty operations are mapped, and an analytical phase during which FDD algorithms are formulated. Kim et al. (2006) documented performance of the cooling mode fault-free and faulty heat pump operation, while this report describes the development of FDD concepts and their analytical implementation.

* Corresponding author. Tel.: +82-2-820-5973; fax: +82-2-3280-5867
E-mail address: minsungk@cau.ac.kr

These techniques typically produce the reference data under the combinations of test conditions which were modulated in laboratory. However, it is very difficult to produce a set of reference data in field systems since the configurations of heat pumps are different. From this end, a machine learning algorithm is introduced in this study to produce the reference model out of field operating data of a heat pump system. The reference model was generated at steady states. To generate machine learning procedure, two environmental chambers were programmed randomly reflecting field environment.

2. Steady State Modeling of Heat Pumps

In this study, the fault detection and diagnosis (FDD) process was envisioned to be performed every time the system is in steady state. Steady state can be detected by observing global system characteristics, e.g., capacity, or – more simply – by monitoring selected parameters. The concept of the steady-state detector originates from noise filter theory. When a system is not steady, thermodynamic system parameters are highly unstable. The variance, or standard deviation, of important parameters is typically utilized to indicate the statistical spread within the data distribution and can be used to characterize random variation of the measured signals.

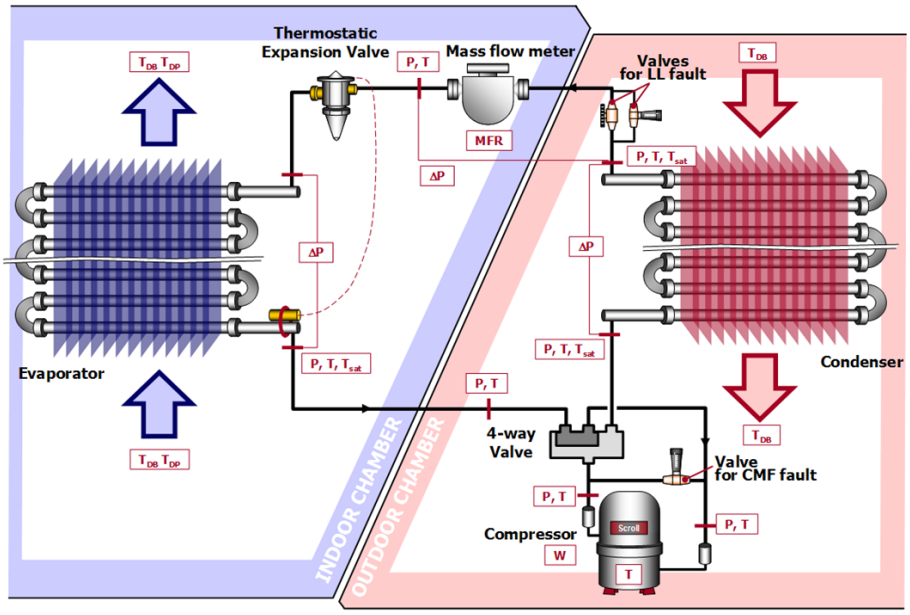


Fig. 1 Schematic diagram of an experimental setup for a residential heat pump in cooling mode

2.1. Determination of characteristic variables

In Fig. 1, typical vapor compression cycle is plotted on Temperature-entropy diagram. In field application, since temperature measurements are most suitable and costly effective, the seven parameters were selected as characteristic variables. The selected seven features are; Evaporator exit refrigerant saturation temperature (T_E), evaporator exit refrigerant superheat (T_{sh}), condenser inlet refrigerant saturation temperature (T_C), compressor discharge refrigerant temperature (T_D), condenser exit liquid line refrigerant subcooled temperature (T_{sc}), evaporator air temperature change (ΔT_{EA}), and condenser air temperature change (ΔT_{CA}).

As inputs of the characteristic variables, three parameters were chosen; outdoor dry-bulb temperature (T_{OD}), indoor dry-bulb temperature (T_{ID}), and indoor dew point temperature (T_{IDP}). The reference model was developed with the 3 independent variables and the 7 dependent variables.

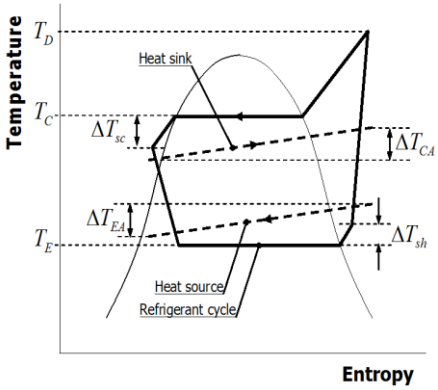


Fig. 2 Temperature-entropy diagram of a vapor compression heat pump system

The temperature sensors are T-type thermocouples with 0.5℃ of uncertainties. Although the above features are limited only by 7 points and the temperature sensors are with relatively large uncertainties, limited measurements are maintained to reflect field measurements.

2.2. Mathematical formulation of the reference models

According to the features defined above, the variables were regressed upon the database generated from the experiments. Equations below show a general form of the regressed equations for the i^{th} feature (or i^{th} dependent variable) as the 1st, 2nd, and 3rd order multivariate polynomial regression (MPR) models, respectively.

$$\phi_i^{(1)} = a_0 + a_1 T_{\mathrm{OD}} + a_2 T_{\mathrm{ID}} + a_3 T_{\mathrm{IDP}} \tag{1}$$

$$\phi_i^{(2)} = \phi_i^{(1)} + a_4 T_{\mathrm{OD}}{}^2 + a_5 T_{\mathrm{ID}}{}^2 + a_6 T_{\mathrm{IDP}}{}^2 + a_7 T_{\mathrm{OD}} T_{\mathrm{ID}} + a_8 T_{\mathrm{ID}} T_{\mathrm{IDP}} + a_9 T_{\mathrm{IDP}} T_{\mathrm{OD}} \tag{2}$$

$$\begin{aligned}\phi_i^{(3)} = \phi_i^{(2)} &+ a_{10} T_{\mathrm{OD}}{}^3 + a_{11} T_{\mathrm{ID}}{}^3 + a_{12} T_{\mathrm{IDP}}{}^3 + a_{13} T_{\mathrm{OD}} T_{\mathrm{ID}} T_{\mathrm{IDP}} + a_{14} T_{\mathrm{OD}}{}^2 T_{\mathrm{ID}} + a_{15} T_{\mathrm{OD}}{}^2 T_{\mathrm{IDP}} + a_{16} T_{\mathrm{ID}}{}^2 T_{\mathrm{OD}} + a_{17} T_{\mathrm{ID}}{}^2 T_{\mathrm{IDP}} \\ &+ a_{18} T_{\mathrm{IDP}}{}^2 T_{\mathrm{OD}} + a_{19} T_{\mathrm{IDP}}{}^2 T_{\mathrm{ID}}\end{aligned} \tag{3}$$

From the above equations, residuals of the characteristic parameters can be obtained. After the residuals are measured from the system, FDD process identifies defects of the system by analyzing the residuals with thresholds value which determine the system status.

2.3. Machine learning process

Once the steady-state is identified, key performance parameters were evaluated from the references. We validated measured COP and heat capacity by comparing the manufacturer's data. If there is no manufacturer's data, the system with no fault incorporated was pre-operated to evaluate the reference operation of the system. Once the key parameters are evaluated as no fault operation, the measured features are used to train the refrence module. When the COP or heat capacity is out of range from the reference value, the system is regarded in faulty status and FDD procedure is carried out.

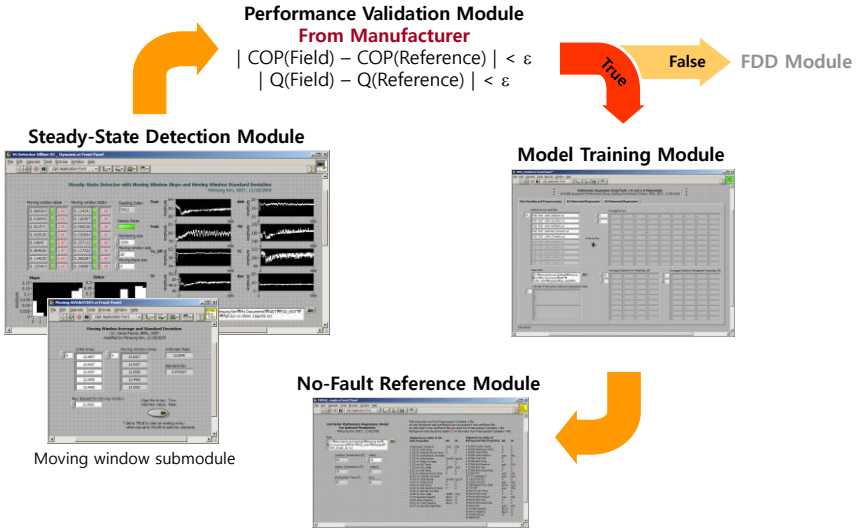


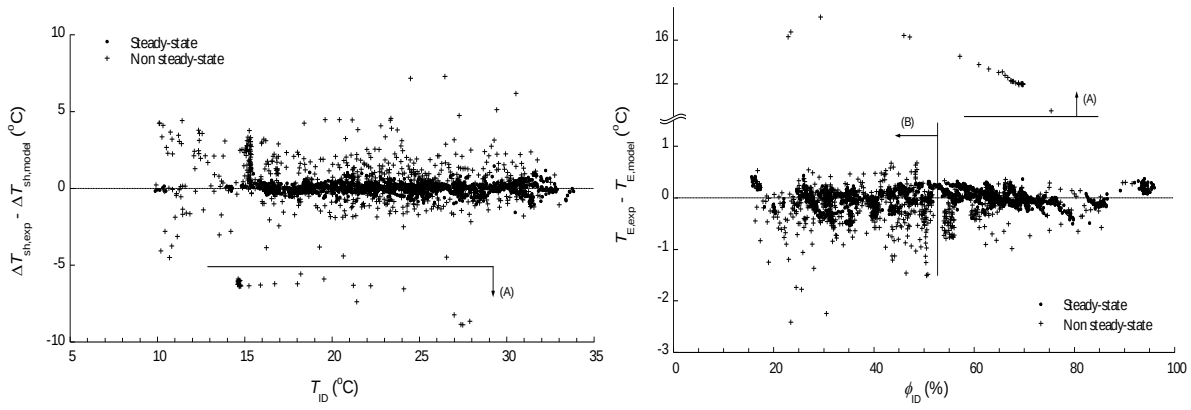
Fig. 3 Machine learning procedure of no fault reference model

3. Validation of the Machine Learning Based Reference Model

Fig. 4 show sample feature residuals as a function of indoor temperature and relative humidity. In Fig. 4, all of the non-steady-state data having large deviation from the reference were filtered out. For both figures, zone A represents the non-steady-state data filtered out during the startup transient. In the low humidity area of Fig. 4(b), marked as zone B or '*TXV hunting*,' highly fluctuating data were filtered out by the steady-state detector. Since the evaporator capacity is reduced for dry inlet air conditions, refrigerant exiting the evaporator oscillates between saturated and superheated. These abrupt condition changes at the evaporator exit cause TXV hunting. When the TXV hunting occurs, other temperatures, especially on the evaporator side, also oscillate within a large range. The no-fault model would thus estimate the parameters inaccurately due to a lack of steady-state data in that range. Once the model estimations are acceptable for other conditions, there is no reason to set the steady-state thresholds so low as to filter all the oscillating data out. By including some data in this oscillating zone within a no-fault model, we can obtain a model that covers a wider range of operating conditions.

3.1. Uncertainties due to steady-state variation and lack of measurement repeatability

To determine a realistic value of the threshold, validation of the measurements is mandatory. Naturally, the system measurements have uncertainties due to sensors – mostly thermocouples – and due to lack of measurement repeatability. The uncertainty of a thermocouple may come from measurement noise and drift. Considering the measurement noise behaves like zero-mean white noise, its natural variation can be characterized closely by the steady-state standard deviation, $\sigma_{i,SS}$, defined in Chapter 3. Thermocouple drift is the measurement bias that varies over longer time periods than noise. However, the thermocouple drift can be regarded as negligible in this research since the same built-in sensors are used for model development and application to the tested system for FDD, thus their bias has been considered in the reference model measurements for this investigation. To observe the repeatability of the system measurements, we analysed 38 repetitive tests of Kim et al. (2006). The feature standard deviations from repeatability tests, $\sigma_{i,Repeat}$, are listed in Table 1. Table 1 gives us the measurement uncertainty due to steady-state variation, $\sigma_{i,SS}$, and due to variation from test-to-test (measurement repeatability), $\sigma_{i,Repeat}$, for similar test conditions. These two values will be used to calculate total residual threshold uncertainty for each feature.



(a) Residual of T_{sh} vs. T_{ID} (b) Residual of T_E vs. indoor relative humidity

Fig. 4 Results filtered by the steady-state detector on the plots with feature residuals and independent variables (zone A: startup transient, zone B: TXV hunting)

Table 1 Standard deviation of the selected features

Units of °C		T_{sh}	T_{sc}	T_E	T_D	T_C	ΔT_{CA}	ΔT_{EA}
Steady-state standard deviation	$\sigma_{i,SS}$	0.124	0.052	0.024	0.058	0.035	0.063	0.058
Stdev. from repeatability tests	$\sigma_{i,Repeat}$	0.101	0.156	0.084	0.280	0.166	0.088	0.111

3.2. Uncertainties due to the reference models

Since measurements are used with the reference model predictions to determine residuals, the square-root of the sum of residuals presents a non-Gaussian RMS error. Thus we analyse the no-fault measurements distribution in detail to provide the methodology for determining a proper value of the threshold ε_i. In most cases, it is hard to obtain a reference model covering all operating conditions. To train a reference model after installation, a real-time decision of fault-free or faulty status is mandatory. In contrast to the steady-state and repetition uncertainty, the model uncertainty comes from the imperfections associated with any mathematical model. We define average bias of the model estimation as the averaged residual between the model and current measurement in no zero-mean noise. The model standard deviation, $\sigma_{i,Model}$, characterizes the model uncertainty. Since the zero-mean noise uncertainty($\sigma_{i,SS}$) and model uncertainties($\sigma_{i,Model}$) amplify the variability of residuals independently, it is reasonable to assume that no joint effect exists between the two uncertainties. Therefore, the covariance between the two uncertainties($\sigma_{i,SS} \cdot \sigma_{i,Model}$) is zero, and $\sigma_{i,NF}$ will be a squared sum of $\sigma_{i,SS}$ and $\sigma_{i,Model}$ as shown below. By combining the equation with Table 1, $\sigma_{i,Model}$ can be estimated in Table 2.

$$\sigma_{i,NF} = \sqrt{\sigma_{i,SS}^2 + \sigma_{i,Model}^2} \tag{5}$$

Table 2 Net model uncertainties of the features using the 1st, 2nd, and 3rd order MPR models

Model uncertainties, $\sigma_{i,Model}$ (°C)	T_{sh}	T_{sc}	T_E	T_D	T_C	ΔT_{CA}	ΔT_{EA}
1st order MPR model	0.557	0.244	0.549	0.799	0.179	0.150	0.581
2nd order MPR model	0.328	0.197	0.147	0.319	0.047	0.040	0.131
3rd order MPR model	0.197	0.133	0.123	0.250	0.029	0.019	0.071

4. Determination of No Fault Threshold

We observed uncertainties from the no-fault measurements. Considering that total uncertainty is due to steady-state uncertainty, modeling uncertainty, and lack of measurement repeatability uncertainty, the threshold is proportional to the total uncertainty as shown below, where the constants k_1, k_2, and k_3 define the confidence intervals for each uncertainty. Depending on the confidence level, the constants k_1, k_2, and k_3 can be determined based on the distribution for each uncertainty term.

$$\varepsilon_i = \sqrt{\left(k_1 \frac{\sigma_{i,\mathrm{SS}}}{\sqrt{n}}\right)^2 + \left(k_2 \sigma_{i,\mathrm{Model}}\right)^2 + \left(k_3 \sigma_{i,\mathrm{Repeat}}\right)^2} \tag{6}$$

4.1. Confidence interval, k_1, for the steady-state uncertainty

Since we use measurements and standard deviations in a preset moving window, their distribution depends on the characteristics of the moving window. When *n* no-fault data are sampled from a Gaussian distribution with standard deviation, σ_i, the quantity *t* can be defined below, where μ_i is the current mean of the moving window of *n* samples. In such a case, *t* follows a Student's *t*-distribution with *n* – 1 degrees of freedom.

$$t = \frac{x_i - \mu_i}{\sigma_i / \sqrt{n}} \tag{7}$$

When we set a $1 - \alpha$ probability that the two values are equal ($x_i = \mu_i$), the confidence interval, $k_1 = t_{\alpha/2,\, n-1}$, is described as below where $t_{\alpha/2,\, n-1}$ is a two-sided confidence interval.

$$P\left(\left|x_i - \mu_i\right| < t_{\alpha/2,n-1} \frac{\sigma_i}{\sqrt{n}}\right) = 1 - \alpha \tag{8}$$

With a $1 - \alpha = 99$ % confidence, $t_{0.005,9} = 3.25$ which is larger than Gaussian distribution of 2.58. Table 3 shows the values of $k_1 = t_{\alpha/2,\, 9}$. For 99 % confidence (or credibility) level, k_1 is 3.25.

Table 3 Two-sided confidence intervals with degrees of freedom of four and nine

$1 - \alpha$ (%)	80.0	90.0	95.0	99.0
$\alpha/2$ (%)	10.0	5.0	2.5	0.5
$t_{\alpha/2,4}$[1]	1.533	2.132	2.776	4.604
$k_1 = t_{\alpha/2,9}$[2]	1.383	1.833	2.262	3.250

[1] 5 sample moving window
[2] 10 sample moving window

4.2. Confidence interval, k_2 , for model uncertainty

Figure 5 shows the distribution of the T_{sh} residual using the 3rd order MPR model applied to the NFSS data discussed in Chapter 4. As seen in the plot, a Gaussian assumption tracks the residual distribution of the feature to a certain extent. However, residuals near zero are distributed narrower than a Gaussian. At high residual values where $|\, r(T_{\mathrm{sh}})\,| > 3$ °F, a Gaussian assumption underestimates the probability. From the Gaussian approach, 99 % of data fall within the range of ±1.08 °F, but no-fault test data have a wider range of ±1.41 °F to cover 99 % of all data.

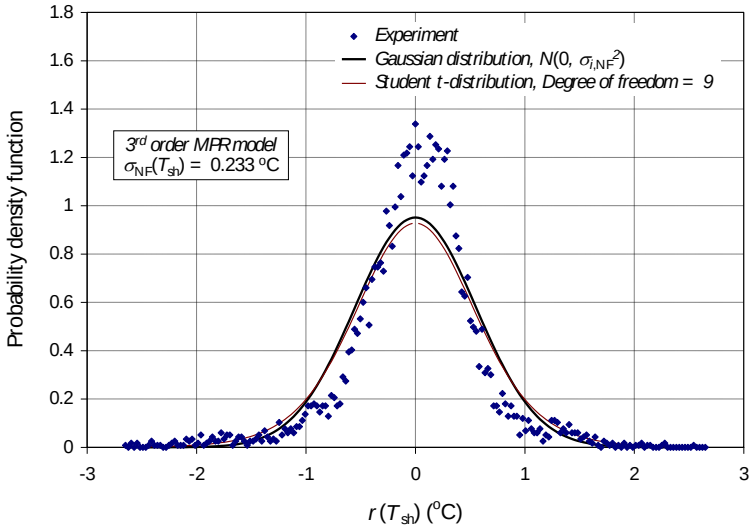


Fig. 5 Comparison of the distributions of the T_{sh} residuals from no fault experimental data and 3rd order MPR model based on the model RMS error; Gaussian distribution, student *t*-distribution, and the calculated distribution from the test data.

Table 4 Two-sided confidence interval of the seven features for the 3rd order MPR model

$1-\alpha$ (%)		75.0	97.5	99.5
$k_2 = t_{\alpha/2,\, n-1}$	T_{sh}	1.00	2.26	2.96
	T_{sc}	0.93	2.22	3.37
	T_E	1.10	2.06	2.65
	T_D	1.15	1.96	2.63
	T_C	1.03	2.03	3.03
	ΔT_{CA}	1.14	1.95	2.64
	ΔT_{EA}	0.95	2.16	3.22

4.3. Confidence interval, k_3 , for lack of measurement repeatability

Repetitive measurements of a random variable will follow a Gaussian distribution, thus, under similar measurement conditions, repetitively measured feature residuals will also follow a Gaussian distribution. Table 5 shows the confidence interval with regard to the confidence level for a Gaussian distribution at various confidence levels. For example, with 99 % credibility, k_3 equals 2.576. From the confidence intervals k_1, k_2, and k_3 obtained above, Table 5 is calculated for the feature thresholds with 50 %, 95 % and 99 % credibility for the moving window size of 5 and 10 samples.

Table 5 Feature thresholds at different confidence levels for two sample sizes

(a) Moving window of 5 samples

Threshold of the features	T_{sh}	T_{sc}	T_E	T_D	T_C	ΔT_{CA}	ΔT_{EA}
50 % credibility, $\varepsilon_{i,0.50}$ (°C)	0.131	0.134	0.092	0.243	0.082	0.064	0.086
95 % credibility, $\varepsilon_{i,0.95}$ (°C)	0.504	0.413	0.324	0.756	0.239	0.192	0.274
99 % credibility, $\varepsilon_{i,0.99}$ (°C)	0.758	0.579	0.426	0.987	0.317	0.265	0.383

(b) Moving window of 10 samples

Threshold of the features	T_{sh}	T_{sc}	T_E	T_D	T_C	ΔT_{CA}	ΔT_{EA}
50 % credibility, $\varepsilon_{i,0.50}$ (°C)	0.130	0.134	0.092	0.243	0.082	0.064	0.086
95 % credibility, $\varepsilon_{i,0.95}$ (°C)	0.496	0.411	0.323	0.755	0.237	0.187	0.271
99 % credibility, $\varepsilon_{i,0.99}$ (°C)	0.735	0.574	0.424	0.983	0.313	0.248	0.373

5. Conclusion

In this study, we developed no fault reference model of vapor compression heat pump by machine learning process with statistical evaluations. Characteristic variables were assumed to behave independently, and uncertainties were estimated in three different ways; steady-state uncertainty, repeatability uncertainty, and reference model uncertainty. From the analysis, we obtained each uncertainty and thresholds depending on the credibility. Distribution of residuals was unique compared to typical Gaussian or student *t*-distribution, especially larger residuals. To reduce uncertainty that may be occurred by the large residuals, it is necessary to increase threshold values to minimize false detection.

Acknowledgements

This paper is jointly supported by Korea Institute of Energy Technology Evaluation and Planning (KETEP) (No. 20168510011420) and by Korea Evaluation Institute of Industrial Technology (KEIT) (No. 10063187) funded from Ministry of Trade, Industry and Energy.

References

[1] Proctor, J., 2004, "Residential and small commercial central air conditioning; Rated efficiency isn't automatic," Presentation at the Public Session. ASHRAE Winter Meeting, Jan. 26, Anaheim, CA.
[2] Breuker, M. S., Braun, J. E.. 1998, "Evaluating the performance of a fault detection and diagnostic system for vapor compression equipment," Int. J. of HVAC&R Research, Vol. 4, No. 4, pp. 401-425.
[3] Kim, M., Payne, W. V., Domanski, P. A., and Hermes, C. J. L.. 2006, "Performance of a residential heat pump operating in the cooling mode with single faults imposed," NISTIR 7350, National Institute of Standards and Technology, Gaithersburg, MD, USA.
[4] Rossi, T. M., 1995, Detection, diagnosis, and evaluation of faults in vapor compression cycle equipment, Ph.D. Dissertation, Purdue Univ., West Lafayette, IN, USA.
[5] Glass, A. S., Gruber, P., Roos, M., and Tödtli, J.. 1995, "Qualitative model-based fault detection in air-handling units," IEEE Control Systems Magazine, Vol. 15, No. 4, pp. 11-22.
[6] Li, H., 2004, A decoupling-based unified fault detection and diagnosis approach for packaged air conditioners, Ph.D. Dissertation, Purdue Univ., West Lafayette, IN, USA.
[7] Kim, M, Payne, W. V., Domanski, P. A., and Yoon, S. H., 2008, "Design of a steady-state detector for fault detection and diagnosis of a residential air conditioner," Int. J. of Refrigeration, Vol. 31, No. 5, pp. 790-799.
[8] Kim, M., Yoon S. H., Payne, W. V. and Domanski, P. A., 2010, "Development of the reference model for a residential heat pump system for cooling mode fault detection and diagnosis", Journal of Mechanical Science and Technology, Vol. 24, No. 7, pp. 1481-1489.